8

Conductivity and Conductometry

F. James Holler *University of Kentucky, Lexington, Kentucky*

Christie G. Enke *The University of New Mexico, Albuquerque, New Mexico*

Electrochemical cells of all types are composed of various electrically conductive materials. The nature and degree of conductivity of the cell can substantially affect the current through the cell, the electric field strengths throughout the cell, and the transport of charged particles from one cell region to another. Thus the phenomenon of conductance is highly relevant to all nonequilibrium electrochemical techniques. For studies that emphasize interfacial behavior, it is helpful to understand the potential fields and ionic transport that occur in the bulk materials adjoining the interfaces. For the study of bulk electrical properties, factors that affect the accuracy and precision of the conductivity measurement determine the limits of usefulness of conductometric detection and determination.

As we shall see, the solution conductivity depends on the ion concentration and the characteristic mobility of the ions present. Therefore, conductivity measurements of simple, one-solute solutions can be interpreted to indicate the concentration of ions (as in the determination of solubility or the degree of dissociation) or the mobility of ions (as in the investigations of the degree of solvation, complexation, or association of ions). In multiple-solute solutions, the contribution of a single ionic solute to the total solution conductivity cannot be determined by conductance measurements alone. This lack of specificity or selectivity of the conductance parameter combined with the degree of tedium usually associated with electrolytic conductivity measurements has, in the past, discouraged the development of conductometry as a widespread electroanalytical technique. Today, there is a substantial reawakening of interest in the practical applications of conductometry. Recent electronic developments have resulted in automated precision conductometric instrumentation and applications are being developed in which conductometry is used to follow the course of highly specific chemical reactions or varying solute concentrations for chromatographic detection.

In this chapter we take a careful look at the phenomenon of electrical conductivity of materials, particularly electrolytic solutions. In the first section, the nature of electrical conductivity and its relation to the electrolyte composition and temperature is developed. The first section and the second (which deals with the direct-current contact methods for measuring conductance) introduce the basic considerations and techniques of conductance measurement. This introduction to conductance measurements is useful to the scientist, not only for electrolytic conductance, but also for understanding the applications of common resistive indicator devices such as thermistors for temperature, photoconductors for light, and strain gauges for mechanical distortion. The third section of this chapter describes the special techniques that are used to minimize the effects of electrode phenomena on the measurement of electrolytic conductance. In that section you will encounter the most recent solutions to the problems of conductometric measurements, the solutions that have sparked the resurgent interest in analytical conductometry.

I. SOME BASIC RELATIONSHIPS

A material exhibits the property of electrical conductivity when it contains charged particles that are free to move through the material. When an electrical potential is applied across such a material, the charged particles will experience a force along the field in a direction opposite to their charge. The resulting net motion of the charged particles is an electric current. The greater the current produced by a given electric field, the greater the conductivity of the material. Since conductivity is related to the rate of flow of charge in response to an electric field, the magnitude of the conductivity is dependent on the concentration, mobility, and charge of the charged particles. In this section, the relationship between the conductivity and the mobility, charge, and concentration of the charged species is developed. Finally, the property of conductivity is related to the measured parameter, conductance.

A. Conductivity

When a charged particle i (an electron or ion) in a liquid or solid material is subjected to an electric field, it quickly reaches a limiting average velocity of motion in the direction of the field opposite to the sign of its charge. The velocity v_i (cm/s) is given by

$$v_i = u_i \mathcal{E} \tag{8.1}$$

where u_i is the particle's mobility and $\mathcal{E}$ is the electric field strength (V/cm). The resulting electric current density (J_i in C/s-cm^2) is given by

$$J_i = v_i N_i q_i \tag{8.2}$$

where N_i is the number of i particles per cubic centimeter and q_i is the coulombic charge on each particle. Note that the sign of v_i will change with the sign of q_i so that J is positive for particles of either sign. Substituting Equation 8.1 in Equation 8.2, we obtain

$$J_i = \mathcal{E} N_i |q_i| u_i \tag{8.3}$$

where the absolute value of q_i is required since the vector quantity v_i has been eliminated.

B. Ionic Conductivity

The total current density J is the sum of the individual current density charge carriers in the substance.

$$J = \sum_{i=1}^{n} J_i = \mathcal{E} \sum_{i=1}^{n} N_i |q_i| u_i \tag{8.4}$$

The electrical conductivity K has been defined as the current density per unit electric field, that is,

$$K \equiv \frac{J}{\mathcal{E}} \tag{8.5}$$

Combining Equations 8.4 and 8.5, we have

$$K = \sum_{i=1}^{n} N_i |q_i| u_i \tag{8.6}$$

From Equation 8.6 it is clear that any change in the substance that affects the concentration or mobility of any of the charge carriers affects the conductivity of the substance. Ionic concentration can be affected by shifts in chemical equilibrium between charged and uncharged species (such as a weak acid and the weak acid anion) or among variously charged species (such as a metal cation with a varying number of anionic ligands). Shifts in chemical equilibrium can be caused by titration with a reaction, or by changes in ionic strength, solvent, or temperature. These latter factors also affect the ionic mobility in significant and complex ways.

In chemical applications, the concentration units of mol/L are more useful than ions/cm^3. From Equation 8.3 and the relationship $N_i = C_i N_{av}/1000$, where C_i is the molar concentration of i and N_{av} is Avogadro's number,

$$J_i = \mathcal{E}\frac{C_i N_{av}}{1000}|q_i|\,u_i \tag{8.7}$$

The charge on an ion q_i can be given by $q_i = Z_i q_e$, where Z_i is the charge number of the ion and q_e is the unit electron charge in coulombs. Also, the quantity $N_{av}q_e$ is defined as the faraday, F. Thus $|q_i| = |Z_i|\ F/N_{av}$. The individual ion current density can now be written

$$J_i = \mathcal{E}\frac{C_i F_{av}}{1000}|Z_i|u_i \tag{8.8}$$

and the conductivity, considering all species, is

$$K = \frac{F}{1000}\sum_{i=1}^{n} C_i|Z_i|u_i \tag{8.9}$$

In the case of a dissolved simple salt, the mobile charges are the cations and anions resulting from the solvation and dissociation of the salt. The conductivity is thus

$$K = \frac{F}{1000}\left(C_+|Z_+|u_+ + C_-|Z_-|u_-\right) \tag{8.10}$$

Electrical neutrality requires that the charge concentration for positive and negative charges be equal, that is,

$$C_+|Z_+| = C_-|Z_-| \tag{8.11}$$

If the salt is *completely* dissociated, the normality of the salt solution, C*, is equal to $C_+ |Z_+| = C_- |Z_-|$. The equivalent conductance Λ of a salt solution is defined as

$$\Lambda = \frac{1000K}{C^*} \tag{8.12}$$

whether the salt is completely dissociated or not. In Equation 8.12, C* is the normality of the salt solution, *not* just the concentration of the ions. Clearly, Λ depends on the degree of dissociation of the salt, having a lower value for a lower degree of dissociation. The dissociation reaction can be studied by measuring Λ as a function of C* [1,2].

The definition in Equation 8.12 does not require complete dissociation, but *if the salt is completely dissociated*, from Equation 8.10,

$$K = \frac{C^*F}{1000}(u_+ + u_-) \quad \text{complete dissociation} \tag{8.13}$$

Combining Equations 8.12 and 8.13 gives us

$$\Lambda = F(u_+ + u_-) \quad \text{complete dissociation} \tag{8.14}$$

Now the ionic equivalent conductance λ can be defined for each ion.

$$\lambda_+ \equiv Fu_+ \qquad \lambda_- \equiv Fu_- \qquad \lambda_i \equiv Fu_i \tag{8.15}$$

Substituting the expressions for λ_+ and λ_- into Equations 8.13 and 8.14, we have, for the case of complete dissociation,

$$K = \frac{C^*}{1000}(\lambda_+ + \lambda_-) \quad \text{complete dissociation} \tag{8.16}$$

and

$$\Lambda = \lambda_+ + \lambda_- \quad \text{complete dissociation} \tag{8.17}$$

Since λ depends on the mobility of the ion, it is a function of the ion type and of the solution parameters (solvent, solute concentration, temperature, etc.). At very low solute concentrations, λ reaches a steady "limiting" value, λ^0, that is often tabulated for the common ions in water solvent at specific temperatures. A table of λ^0 values is given in Table 8.1. The λ^0 values from such a table can be used to estimate the conductivity of a completely dissociated salt solution by application in Equation 8.10. For finite salt concentrations, the calculated values are indicative, but not exact. Onsager, Fuoss, and others [2,3] have developed equations by which quite accurate values of λ can be calculated from λ^0 values under certain circumstances.

In analytical applications of conductometry, the sample often contains many species of ions, each contributing to the total conductivity. The total conductivity is then

$$K = \frac{1}{1000}\sum_{i=1}^{n} C_i^*\lambda_i = \sum_{i=1}^{n} C_i|Z_i|\lambda_i \quad \begin{array}{l}\text{complete dissociation or}\\ \text{actual ion concentrations}\end{array} \tag{8.18}$$

where C_i^* and C_i are the normality and molarity, respectively, of the ionic species i in the solution. Thus, in using Equation 8.18 to calculate (or estimate) the conductivity of a solution, *all* ionic species present must be included. Also, Equation 8.18 shows that the variation in concentration or mobility of any of

Table 8.1 Limiting Equivalent Conductance of Ions in Water at 25°C

Cations	λ_+^0	Anions	λ_-^0
H^+	249.8	OH^-	199.2
Li^+	38.6	F^-	55.4
Na^+	50.1	Cl^-	76.4
K^+	73.5	Br^-	78.1
Rb^+	77.8	I^-	76.8
Ag^+	61.9	NO_3^-	71.5
NH^{4+}	73.5	ClO_3^-	64.6
$(CH_3)_2NH_2^+$	51.8	ClO_4^-	67.4
$(CH_3)_3NH^+$	47.2	IO_4^-	54.5
$(CH_3)_4N^+$	44.9	Formate	54.6
Mg^{2+}	53.0	Acetate	40.9
Ca^{2+}	59.5	Benzoate	32.4
Ba^{2+}	63.6	SO_4^{2-}	80.0
Cu^{2+}	53.6	CO_3^{2-}	69.3
Zn^{2+}	52.8	$Fe(CN)_6^{4-}$	111.0
La^{3+}	69.7	—	—
Ce^{3+}	69.8	—	—

Source: Reprinted in part from Reference 2, p. 463, with permission. Copyright 1968 Butterworths.

the ionic species will result in a change in K. A change in temperature can affect both ion concentration and mobility by affecting ion dissociation, complexation, and solvation equilibria as well as solvent viscosity. The combined effects are often complex and rarely negligible.

C. Conductance

When a voltage source of E volts is connected across the contacts of conducting material as shown in Figure 8.1, the mobile charges move in the conducting material in response to the field. The electric field $\mathcal{E}$ applied to the conductor is E/ℓ. From Equation 8.5 the resulting current density J is

$$J = \mathcal{E}K = \frac{EK}{\ell} \tag{8.19}$$

The total current I is current density times the area a:

$$J = Ja = \frac{EKa}{\ell} \tag{8.20}$$

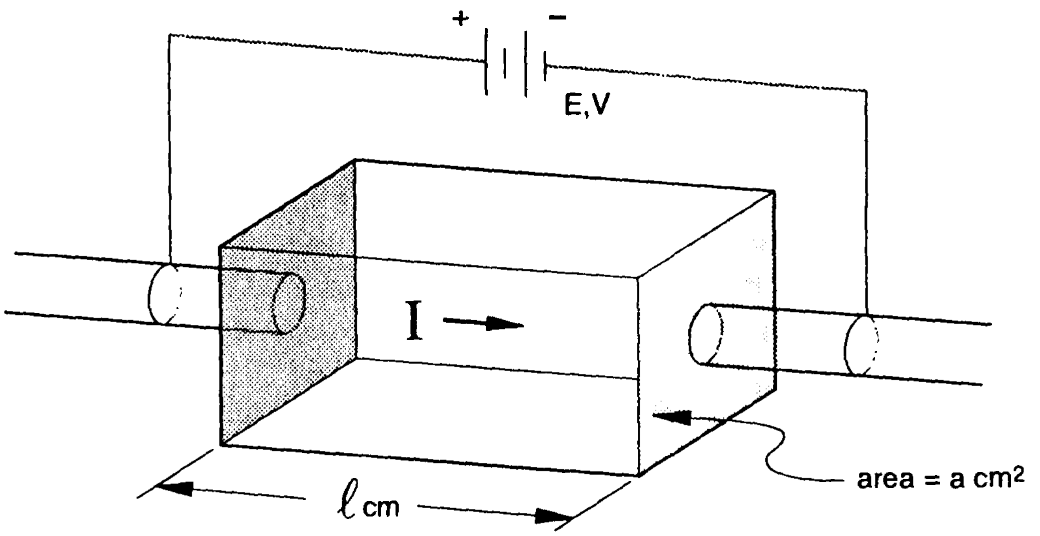

Figure 8.1 The application of an electric field across a conducting material is accomplished by placing the material between metallic contacts and applying an electrical potential to those contacts.

From Equation 8.20 we see that the current in a conductor is proportional to the voltage across it. The proportionality constant Ka/ℓ is defined as the conductance G:

$$G \equiv K\frac{a}{\ell} \tag{8.21}$$

The current-voltage relationship is now simply

$$I = EG \tag{8.22}$$

This relationship was first articulated by Ohm, who also defined the resistance R of a conductor as the reciprocal of the conductance,

$$R \equiv \frac{1}{G} \tag{8.23}$$

so that Ohm's law is also often written

$$I = \frac{E}{R} \quad \text{or} \quad E = IR \tag{8.24}$$

Another way to state Equation 8.24 is that the voltage across a resistor is proportional to the current through the resistor. These simple relationships are the basis of virtually all techniques of measuring conductance (or resistance); the measurement of the I/E ratio for a conductor yields G directly, while the E/I ratio is equal to R. The unit of R (volts/ampere) is the ohm (Ω) and the unit of G (amperes/volt) is the mho (Ω^{-1}).

In the case of electrolytic solutions, it is G that is measured; that is, the conductance of a cell filled with the sample solution. The conductance of an actual cell is related to the conductivity of the solution and the geometry of the cell as given by Equation 8.21. The conductance of the solution is proportional to the area a of the electrodes and inversely proportional to the distance between them, so that K is calculated from a measurement of G by $K = G\ell/a$, where the factor ℓ/a is often called the cell constant. Actually, the exact cell constant is rarely obtained by geometric measurement. It is generally determined empirically by measuring the conductance of a cell filled with a solution for which the conductivity is exactly known.

II. DC CONTACT MEASUREMENT OF CONDUCTANCE

The conductance of some materials can be measured by the scheme shown in Figure 8.1 and Ohm's law. The current can be measured for a given applied voltage, or the voltage across the contacts can be measured when a known current is passed between them. This approach depends on a free and uniform transport of charge carriers through the interface between the metallic contacts and the test material. Since the charge carriers in the metallic contacts are electrons, the material to be tested also needs to be an electronic conductor. Some nonmetallic electronic conductors (such as semiconductors) may require special surface treatments at the contact interface to provide free electronic transport through it. There are, fortunately, many devices, substances, and measurements for which metallic contacts are sufficiently ideal and for which the simple relationships of Ohm's law can be used as the basis of measurement. The ohmmeters and Wheatstone bridge described in the next two parts of this section can be used where the metallic contact is effective. The consideration of special contact problems will conclude this section.

A. Practical Ohmmeters

The resistance measurement concept used in a modern digital ohmmeter (or the "ohms" scales of a digital multimeter) is shown in Figure 8.2. The readout device is a digital voltmeter (DVM) composed of a fixed-range analog-to-digital converter and decimal display. The full-scale reading of the digital voltmeter is frequently 200.0 mV. A switchable constant-current source is applied across the parallel combination of the DVM and the unknown resistance. It is assumed that the DVM input resistance is so much larger than that of the unknown resistance that all of the current passes through the test resistance. If the constant current were exactly 1.000 mA, the voltage at the DVM input would be 1.000

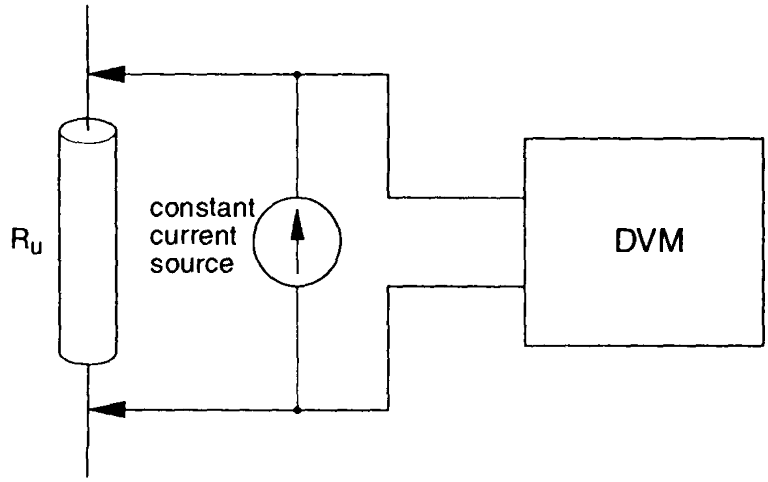

Figure 8.2 The digital ohmmeter uses a constant-current source to produce a voltage across the unknown resistance proportional to its resistance, and a digital voltmeter to read that voltage.

V for each ohm of resistance in the unknown. If the full-scale reading of the DVM were 200.0 mV, the maximum resistance that could be measured would be 200.0 Ω. To measure higher values of resistance, smaller decade values of current are applied; to measure lower values of resistance without loss of significant figures, higher values of current are applied. The overall useful range of this approach is determined on the low end by the contact resistance of the probes and the maximum constant-current source available, and on the high end by the lowest practical constant-current source and highest practical DVM input resistance.

Operational Amplifier Resistance-to-Voltage Converters

For continuous laboratory monitoring of resistance, the operational amplifier current follower circuit offers an easy means of converting either resistance or conductance to a proportional voltage. In Figure 8.3a, R_u is connected to the voltage source E, and the result is a current $i = E/R_u$ that is proportional to the conductance of R_u. The operational amplifier maintains an output voltage such that point S is at the common potential. Therefore, the input current, i, produces a voltage $e_o = iR_u$ at the current-follower output. Also, the connection of G-to-I converter circuit to point S is equivalent to a connection to common; that is, essentially no additional voltage or current is added to the input circuit. Since $i = E/R_u$ and $e_o = -iR_u$,

$$e_o = \frac{-ER_f}{R_u} = -ER_fG_u \tag{8.25}$$

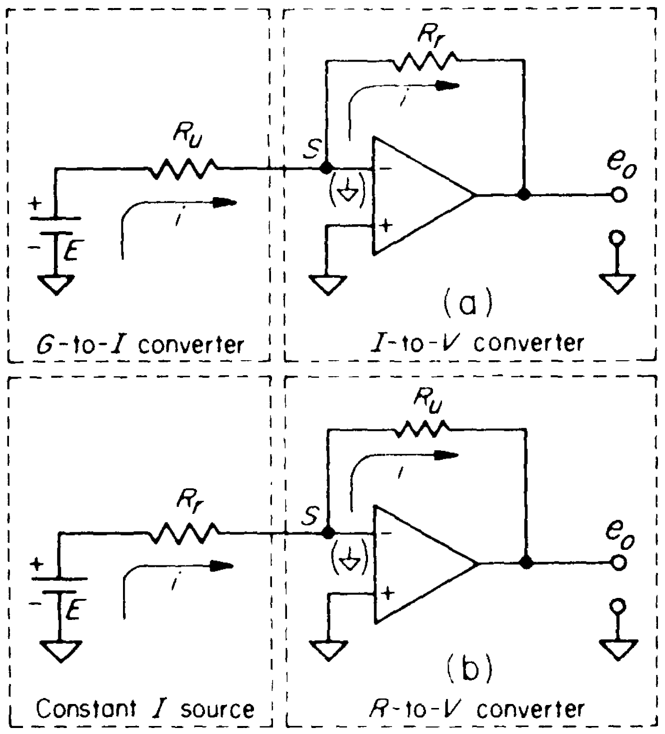

Figure 8.3 Current-follower circuit for resistance measurement: (a) $e_0 = -ER_r/R_u$; (b) $e_0 = -ER_u/R_r$.

This results in an output voltage directly proportional to the conductance of R_u within the output voltage and current capabilities of the operational amplifier.

In the circuit of Figure 8.3b, a fixed resistance R_r is used in the input current-generating circuit. Since this same current passes through R_u and the operational amplifier maintains point S at the common potential, the output voltage e_0 is equal to $-iR_u$. From

$$i=\frac{E}{R_r} \quad \text{and} \quad e_0=-iR_u \tag{8.26}$$

$$e_0=-\frac{E}{R_r}R_u \tag{8.27}$$

A very useful application of the circuit of Figure 8.3b is produced if we replace the feedback resistor R_u with a resistive transducer such as a coated semiconductor thermistor. The commercial availability of small, rapid-response, chemically inert thermistors that have conveniently measurable resistances at temperatures of 200–600 K makes them an excellent choice as the transducer in chemical applications that require the rapid and accurate measurement of temperature. Unfortunately, a continuous current in R_u may produce undesirable

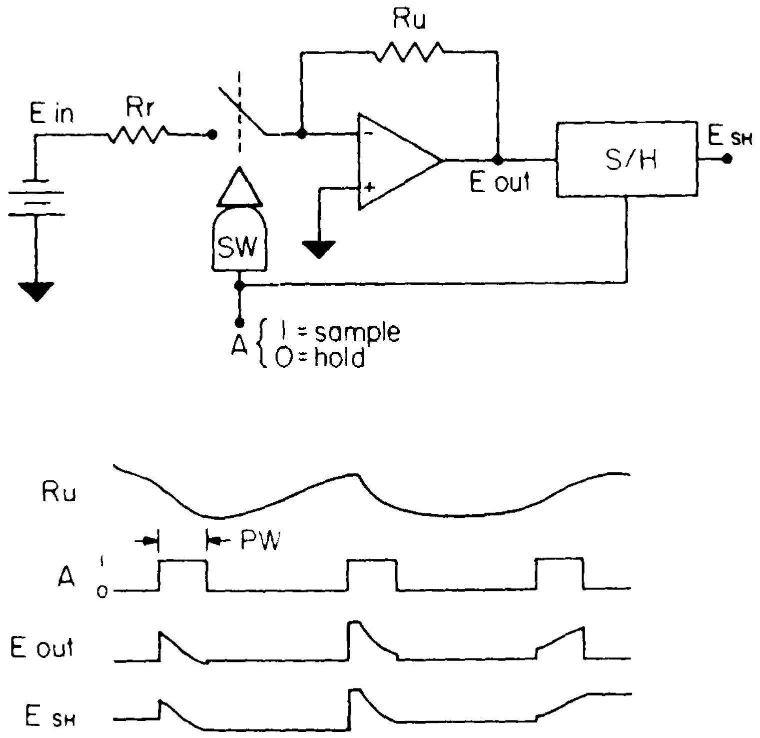

Figure 8.4 Pulsed dc measurement of resistance.

Joule heating in the thermistor and its surroundings and thus cause an error in the measurement. This error may be reduced by utilizing a pulsed voltage source as illustrated in Figure 8.4. The logic signal A closes the electronic switch SW and produces a current pulse in R_u, the duration of which is designated by PW in the figure. The logic signal also switches the sample-and-hold module (S/H) into the sample mode and causes the transient analog signal that is proportional to R_u to be held at the S/H output between pulses. The pulses need only be applied at the frequency of the desired temperature sampling rate and the output of the S/H module may easily be connected to an analog-to-digital converter for computer data acquisition.

B. Null Comparison Measurement

In a null comparison measurement of resistance, the effect of an unknown resistance must be compared with the effect of a variable standard resistance under conditions as identical as possible. Therefore, the unknown and standard resistances are placed in identical circuits in such a way that the resulting voltage or current in each circuit can be compared. Then the standard is varied until the difference in voltage or current between the two circuits is zero. Several methods for performing this comparison have been devised, of which the Wheatstone bridge is by far the most common. Comparison methods for resistance measurement offer great accuracy, resolution, and relative independence of the electronic sources and detectors used.

The Wheatstone Bridge

The Wheatstone bridge shown in Figure 8.5 provides the most direct and best known circuit for comparison of unknown resistances against standard resistances. Resistances R_A, R_B, and R are standard resistance values that are used in the measurement of the unknown resistance R_u. Resistance R is made variable and is adjusted until the null detector indicates that the bridge is balanced.

When the circuit is at balance, there is no current through the null detector and no potential difference between terminals x and y. At balance, four significant conditions exist:

1. The current through R_A and R_u is I_1.
2. The current through R_B and R is I_2.
3. $I_1R_u = I_2R$.
4. $I_1R_A = I_2R_B$.

Therefore, $R_u/R = R_A/R_B$ and

$$R_u = R\frac{R_A}{R_B} \tag{8.28}$$

It can be seen from Equation 8.28 that the unknown resistance R_u is determined from the values of the three standard resistances R, R_A, and R_B. It is common practice to make the ratio R_A/R_B some exact decimal fraction or multiple such as 0.01, 0.1, 10, or 100 and to refer to this ratio as the "multiplier."

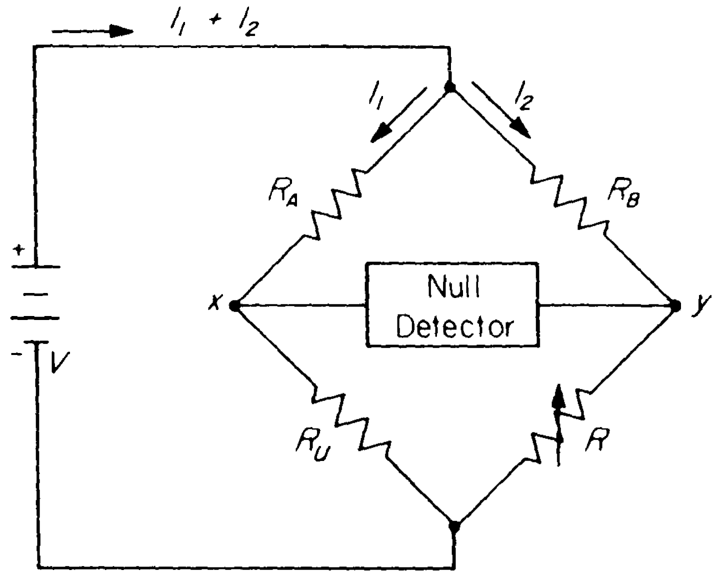

Figure 8.5 Wheatstone bridge.

The resistance R is variable continuously or in small increments so that the dial reading of R times the multiplier setting equals the unknown resistance R_u. The main sources of error in a Wheatstone bridge are the inaccuracies of the three standard resistances R, R_A, and R_B (as low as 0.001%), establishing the null point, and thermal electromotive force (EMF) values.

The magnitude of the off-balance indication of the null detector of a Wheatstone bridge is sometimes used as a measure of the change in resistance of the unknown resistor R_u. In this application, R_u is frequently a light-, temperature-, or strain-dependent resistor. When matched devices are used for R and R_u, or R_A and R_u, an off-balance output is obtained that is related to the ratio of the resistances of the two devices. This "comparative" resistance measurement with matched devices can tend to cancel the effects of resistance changes due to environmental factors other than the measured quantity. For example, the resistance of strain-gauge resistors depends on temperature and humidity as well as strain. If twin strain gauges are used in adjacent arms of a Wheatstone bridge with one gauge under strain but both in the same environment, the environmental effects will not affect the resistance ratio and only the strain effect will affect the off-balance output signal.

C. Contact Considerations

In all the preceding examples of conductance or resistance measurement, it was assumed that the probe leads and the contacts to the measured conductor were ideal. An ideal lead and contact have zero resistance and no thermally generated voltages or uncompensated contact potentials. In a very wide range of measurements of electron-conducting devices, the ideal conditions are met within the desirable or practical error limits. However, the measurement of very low resistances can pose a problem in that the lead and contact resistance must be negligible compared to the resistance measured. Normal lead and contact resistance can be several tenths of an ohm, which limits 1% accuracy measurements to values greater than about 50 Ω.

The best technique for lower resistances is the four-contact method shown in Figure 8.6. The leads and contacts that measure the voltage across the resistor, caused by the current through the resistor, are not the same leads and contacts that supply the current. Since the current does not appear in the voltmeter leads or contacts, no error due to an iR voltage in the voltmeter contacts will occur.

Direct contact techniques do not work with electrolytic solutions. One cannot, for example, measure the resistance of salt water in a cell with an ordinary ohmmeter. This is due to the fact that the mobile charge carriers in an electrolytic solution are ions, not electrons. The conversion of ionic to electronic conduction at the electrode interface can only take place through an electrochemi-

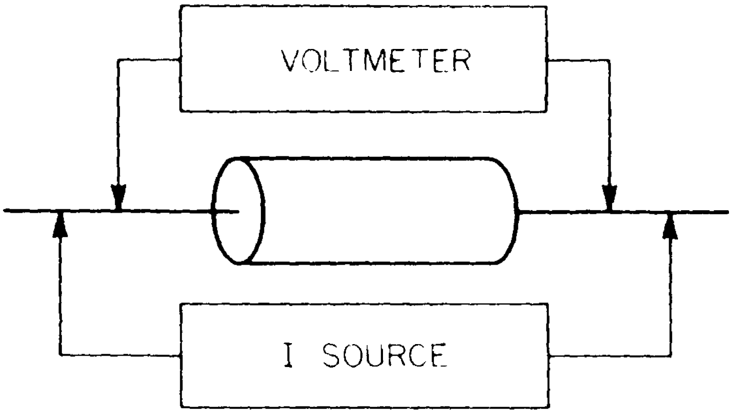

Figure 8.6 Four-contact technique for low-R measurement.

cal oxidation or reduction. The establishment of such a process involves a substantial potential difference between the electrode and the solution and has finite impedance characteristics as well. If the electrodes used to supply the measurement current are separate from the iR drop measuring electrodes, as in the four-electrode scheme described above, the effects of the interfacial reactions at the current electrodes can be minimized. This approach is shown in Figure 8.7. The technique actually measures the conductance of the part of the solution that is in the capillary tubing between the two vials of the H cell. When a current is applied from the current source, this current must appear in the capillary section of the cell. The iR voltage in the capillary section is very much

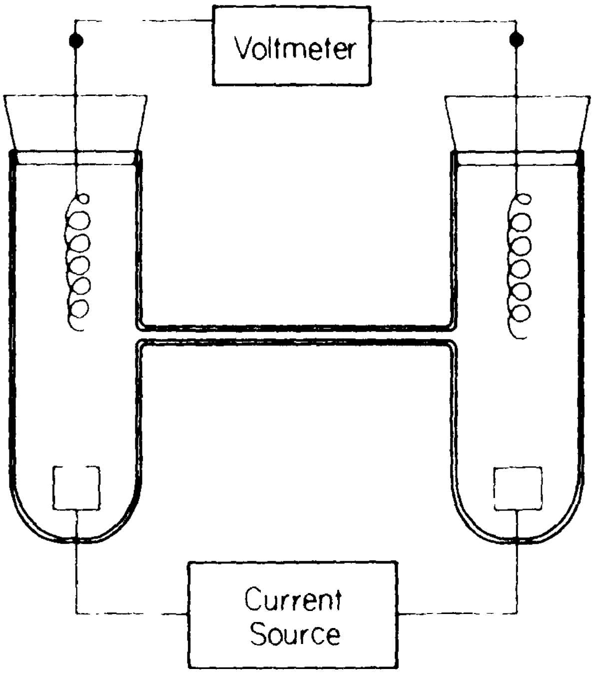

Figure 8.7 Four-contact measurement of electrolytic conductance.

larger than in the vials because of the much smaller cross-sectional area of the capillary. Thus the voltmeter contacts to the solution in the vials measure the voltage (iR drop) developed in the capillary section. If the voltmeter probe contacts have stable and identical electrode-solution potentials, the interface voltages will cancel in the voltmeter circuit. Reference-type electrodes are often used for the voltmeter probes.

III. CAPACITIVE CONTACT MEASUREMENT OF CONDUCTANCE

A method of avoiding the effect of potential differences arising at the electrode-solution interface is to take advantage of the capacitive behavior of the double layer at the electrode surface to make ac (alternating current) contact with the solution. To understand how this may be accomplished, it is necessary to consider a basic model of a conductance cell and examine its behavior under the influence of ac excitation. A review of ac circuit principles at a level sufficient for understanding the behavior of conductance cells and the instrumentation for conductance measurement is presented. The reader who desires a more thorough study of this topic is directed to material contained in the references [4–7].

A. AC Excitation

At relatively low applied frequencies, a conductance cell may be represented as the double-layer capacitance C_s in series with the solution resistance R, as shown in Figure 8.8a. When a sinusoidal voltage e_s is applied to the series RC circuit, the instantaneous current i is the same in every part of the circuit and is given by

$$i = I \sin \omega t \tag{8.29}$$

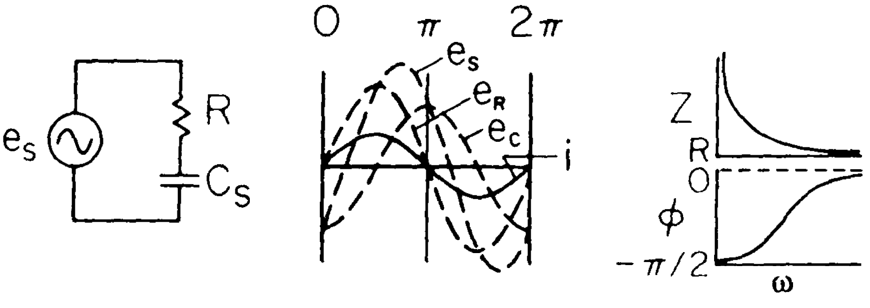

(a) (b) (c)

Figure 8.8 Series RC circuit: (a) circuit; (b) current-voltage relationships; (c) frequency dependence of impedance Z and phase angle ϕ.

where I is the maximum current, ω is the angular frequency (rad/s) ($\omega = 2\pi f$, where f is the frequency in Hz), and t is time (s). From Ohm's law the instantaneous voltage e_R across R is then

$$e_R = iR = IR \sin \omega t \tag{8.30}$$

Since the instantaneous current in a capacitor is given by $i = C_s(de_C/dt)$,

$$e_C = \frac{1}{C_s}\int i\,dt = \frac{1}{C_s}\int I \sin \omega t\,dt \tag{8.31}$$

$$= \frac{I}{\omega C_s}(-\cos \omega t) \tag{8.32}$$

It follows that the maximum voltage E_C across C_s occurs when $-\cos \omega t = 1$ and therefore,

$$E_C = \frac{I}{\omega C_s} = I\frac{1}{\omega C_s} = IX_c \tag{8.33}$$

This expression has a form exactly analogous to Ohm's law in dc circuits. The quantity $1/\omega C_s$ is called the capacitive reactance X_C. It is a measure of the opposition to the flow of charge in a capacitor, and it is therefore measured in ohms. If we now substitute the definition of X_C into the expression for e_C, it follows that

$$e_C = IX_C(-\cos \omega t) \tag{8.34}$$

Finally, applying the appropriate trigonometric identity, we obtain

$$e_C = IX_C \sin\left(\omega t - \frac{\pi}{2}\right) \tag{8.35}$$

A comparison of Equations 8.35 for e_C and 8.30 for e_R reveals two very important points: e_C lags e_R by $\pi/2$ (a quarter cycle or 90° of phase) and e_C is directly proportional to X_C, while e_R is proportional to R.

Capacitive reactance is a frequency-dependent quantity, decreasing with increasing frequency. Typically, double-layer capacitances for aqueous solutions are 10–100 $\mu F/cm^2$. Thus the capacitive reactance for a 1-cm^2 electrode with a 10-μF capacitance at an applied frequency of 10^4 rad/s (1.6 kHz) is

$$X_C = \frac{1}{\omega C} = \frac{1}{(10^4)(10^{-5})} = 10\,\Omega \tag{8.36}$$

The relationships among e_R, e_C, e_s, and i for the series RC circuit are illustrated in Figure 8.8b. Since the instantaneous voltages across R and C are additive, e_s may be obtained by graphically summing e_R and e_C. Note that the current in the circuit is in phase with e_R but is out of phase with e_C by $\pi/2$ (90°), and therefore the signal voltage is always between 0 and 90° out of phase with the current. This phase difference is called the phase angle.

The total opposition to the current in an ac circuit is referred to as its impedance Z, and in a simple RC network is given by the vector sum of R and X_C; that is,

$$Z = \sqrt{X_C{}^2 + R^2} = \sqrt{\left(\frac{1}{\omega C_s}\right)^2 + R^2} \tag{8.37}$$

From the preceding expression and the expressions for e_C and e_R, we see that as the signal frequency is increased, X_C decreases, Z approaches R, and G approaches 1/Z. The potential across C_s also decreases gradually, and the phase angle ϕ between i and e_s approaches zero, as is illustrated in the plot of ϕ versus ω in Figure 8.8c. For an RC circuit, there is a frequency for which X_C = R. The reciprocal of this frequency is called the time constant τ. When $R = 1/\omega C$, $1/\omega = RC$. Thus $\tau = RC$, in seconds.

It is desirable to measure R (and thus G) at a high frequency in order to reduce X_C to a negligible value compared to R. Unfortunately, other complications arise if the frequency is increased above a few kilohertz, and therefore other means must be devised to decrease X_C. A commonly used remedy is to increase the surface area and thus the capacitance of the electrodes as much as possible. A 100-fold area increase is obtained by platinizing the electrodes, that is, electrodepositing a layer of platinum black onto the platinum electrodes, usually from a solution of chloroplatinic acid [8].

A high-frequency limit for the applied potential is encountered above several kilohertz where the impedance of the conductance cell again begins to deviate from the resistance R. Since the solution medium itself is a dielectric situated between two parallel charged surfaces, it can assume the characteristics of a capacitor placed in parallel across the solution resistance as shown in Figure 8.9a. The magnitude of this capacitance is given by

$$C_p = \frac{10^9 D}{4\pi c^2 (l/a)} \tag{8.38}$$

where the quantities D, c, and l/a are the dielectric constant of the medium, the speed of light, and the cell constant, respectively. The dilute aqueous solution dielectric constant D is approximately 80, and if we assume a cell constant of

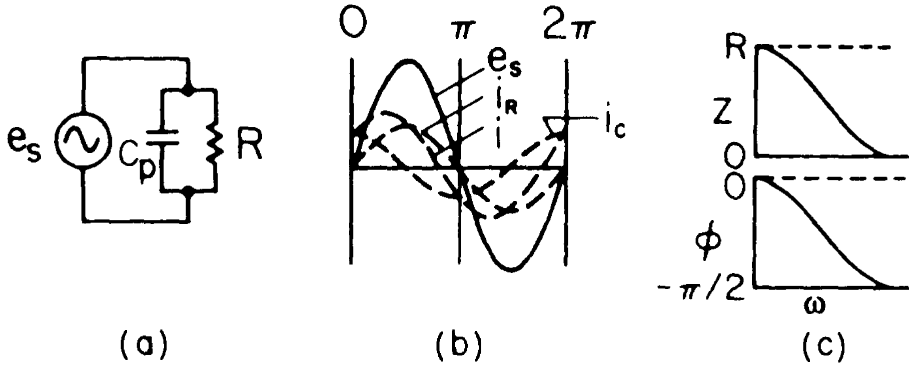

Figure 8.9 Parallel RC circuit: (a) circuit; (b) current-voltage relationships; (c) frequency dependence of impedance Z and phase angle ϕ.

1 cm^{-1}, the parallel capacitance is approximately 10 pF. At an applied frequency of 10^4 rad/s (1.6 kHz) this capacitance results in $X_C = 10\ \text{M}\Omega$.

In order to assess the effect of C_p on the conductance measurements, the analysis of the parallel RC network of Figure 8.9a may be carried out in a manner analogous to the series network discussed previously. The situation differs from the series circuit in that in this case, the *voltage* is the same across R and C_p, and the currents i_C and i_R in C_p and R are different. The instantaneous currents are given by

$$i_C = \frac{e_s}{X_C} \quad \text{and} \quad i_R = \frac{e_s}{R} \tag{8.39}$$

The current in the resistor, i_R, is in phase with the applied voltage while the current in the capacitor leads the applied voltage by 90° as illustrated in Figure 8.9b. To obtain an expression for the total current i, we must find the vector sum of i_C and i_R as follows:

$$i = \sqrt{\left(\frac{e_s}{X_C}\right)^2 + \left(\frac{e_s}{R}\right)^2} = e_s\sqrt{\left(\frac{1}{X_C}\right)^2 + \left(\frac{1}{R}\right)^2} \tag{8.40}$$

The cell impedance is then

$$Z = \frac{e_s}{i} = \frac{1}{\sqrt{(1/X_C)^2 + (1/R)^2}} \tag{8.41}$$

Thus if $X_C \approx 10\ \text{M}\Omega$ as already shown, the current path through C_p only becomes appreciable (for a 1% measurement) when the solution resistance approaches 100 kΩ. Such situations are usually avoided by a judicious choice of cell constant and concentration of electrolyte in the solution of interest.

Unfortunately, other experimental factors, such as contact capacitance at the junction of the cell leads and the measurement system, lead capacitance, and capacitance due to the dielectric properties of the thermostatting medium, may contribute substantially to the parallel capacitance. These effects may be minimized by proper choice of cell design and use of oil rather than water in the thermostatting bath. The art of making ac conductance measurements has been refined to a high degree of precision and accuracy, and detailed discussions of the rather elaborate procedures that are often necessary are available [9,10].

The simple high- and low-frequency models of a conductance cell may be combined in the network shown in Figure 8.10a. The response of this network

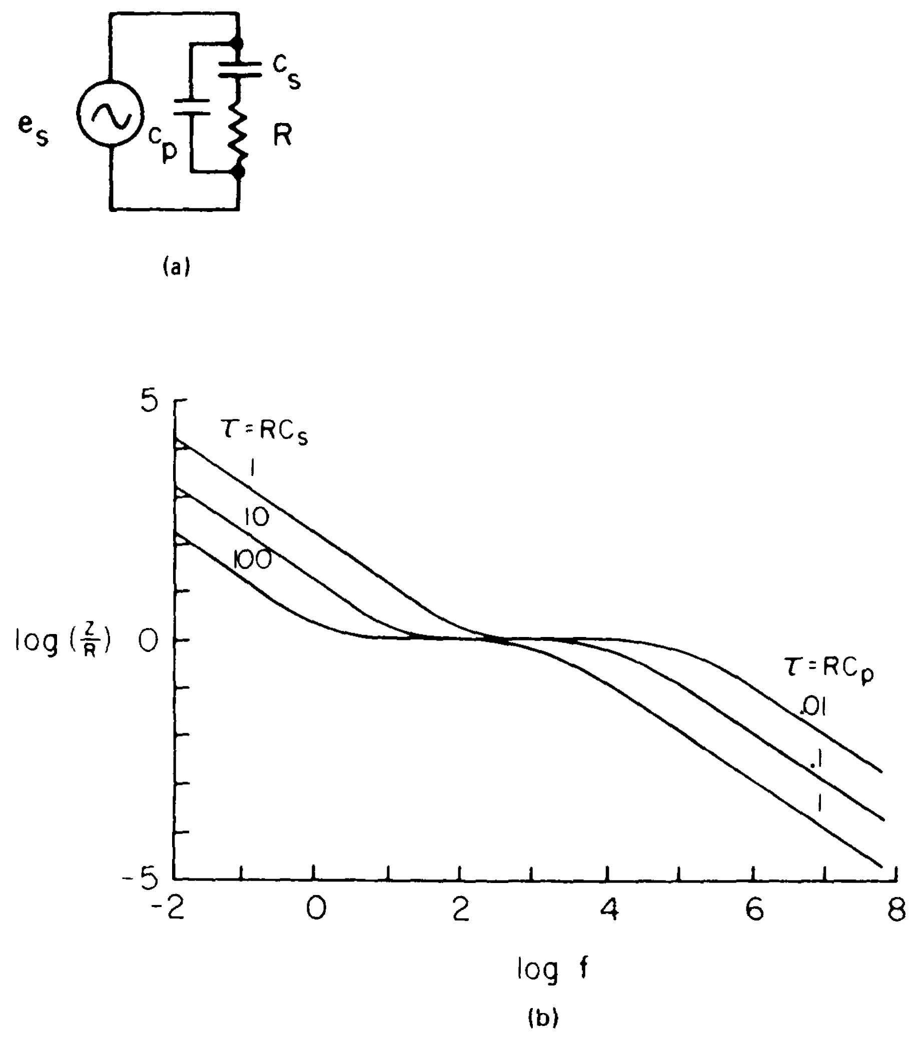

Figure 8.10 Resistance with series and parallel capacitors: (a) circuit; (b) frequency dependence of impedance.

to ac excitation is illustrated in Figure 8.10b, in which the logarithm of the ratio of the total impedance to the resistance is plotted as a function of the logarithm of the frequency for several values of series and parallel RC time constants. It is obvious from the curves that the solution resistance is best measured over a fairly narrow midfrequency range or plateau. For some solutions this plateau may not exist at all. However, if the plateau can be located, the solution resistance is easily determined by measuring the cell impedance as discussed in the following section.

B. Impedance Measurements

It is apparent from the previous discussion that in order to measure electrolytic conductance we must devise a means for compensating for the effects of C_p and C_s. Figure 8.11 illustrates in block diagram form the elements of the impedance measurement process. Basically, a sinusoid is impressed across the conductance cell and the resulting signal is amplified and demodulated in such a way as to produce a signal proportional to the resistive component of the cell impedance. In the last step of the process, the signal is filtered to provide a dc voltage suitable for driving a convenient readout device.

The most straightforward method for measuring impedance is accomplished by choosing an excitation frequency for which $Z = R$ (i.e., $X_{C_s} >> R >> X_{C_p}$), thus making the demodulation step trivial. A very basic circuit for measuring impedance at such frequencies is illustrated in Figure 8.12 [11]. This circuit functions in much the same way as the current-follower circuit of Figure 8.3 except that diodes D_1 and D_2 have been added to rectify (demodulate) the signal resulting from the ac excitation of the cell [12]. As the input signal A drops below zero volts, the summing point of the operational amplifier drops a very small amount below ground potential. This causes the output to swing positive, reverse biasing D_1 and forward biasing D_2, causing the selected feedback resistor, 10R, to be in the feedback loop. At this point, and for the remainder of the negative half-cycle, the gain of the operational amplifier is $10R/Z_{\text{cell}}$.

As the input signal swings above 0 V, the output of the operational amplifier swings negative, causing D_1 to conduct and D_2 to block. This results in a zero-gain situation and the output of the circuit at point B becomes zero. The resulting rectified output is shown in waveform B. This waveform is filtered by the passive RC network at the output to provide a dc signal that may be fed to

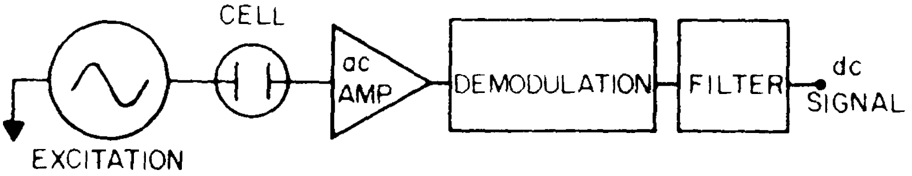

Figure 8.11 Impedance measurement system.

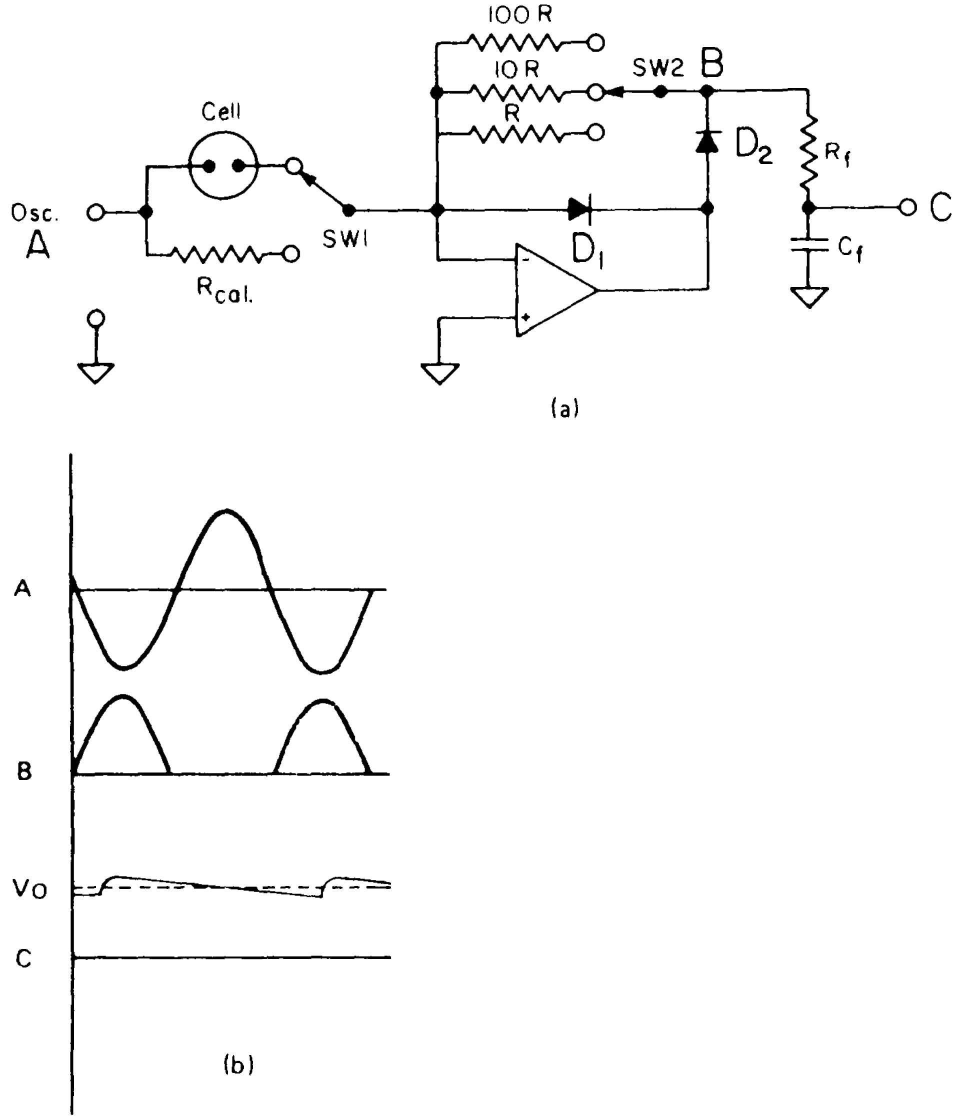

Figure 8.12 Impedance measurement by phase-selective demodulation: (a) circuit diagram; (b) waveforms. [From Ref. 11.]

a strip-chart recorder, digital voltmeter, or other readout device. The switches SW1 and SW2 facilitate calibration of the output and selection of proper amplification for full-scale deflection of the readout device.

Since the output of the circuit is directly proportional to the conductance of the cell ($1/Z_{\text{cell}}$ in this case), the circuit may be used as a direct-reading detector for conductometric titration, reaction kinetic studies of fairly slow reactions, liquid chromatography, or ion-exchange chromatography.

The circuit may be easily constructed for a modest cost using inexpensive operational amplifiers and any of a number of integrated circuit oscillators that are commercially available. This basic piece of instrumentation is suitable for student laboratory experiments, conductometric monitoring of distilled water or other flowing streams, and other routine applications that do not require high precision or absolute accuracy. The instrument is limited to systems in which the capacitive effects are negligible.

Another technique that is useful at frequencies of less than ~10 kHz is phase-selective demodulation. A distinct advantage of this technique is that it enables the separation of the resistive (in-phase or "real") and capacitive (90°-out-of-phase or "quadrature") components of the cell impedance. This is accomplished through the process of cross-correlation [13] (selecting that component of e_s that correlates with the phase of i). The excitation voltage waveform is multiplied by a square wave that is in phase with the cell current waveform.

We can understand how this is carried out by considering the waveforms of Figure 8.13a. At frequencies for which parallel capacitive components of the conductance cell impedance are negligible, sinusoidal excitation of the cell produces the waveforms of A, where e_s, e_R, e_C, and i have the same significance as previously discussed. In order to measure the real component of the impedance, the magnitude of the correlation integral cc must be determined.

$$\mathrm{cc} = \int r e_s \, dt \tag{8.42}$$

The function r is the bipolar square wave illustrated by waveform B, which has an amplitude of unity and is in phase with e_R. We shall demonstrate that the integral of Equation 8.42 is proportional to R over the first half-cycle. As an

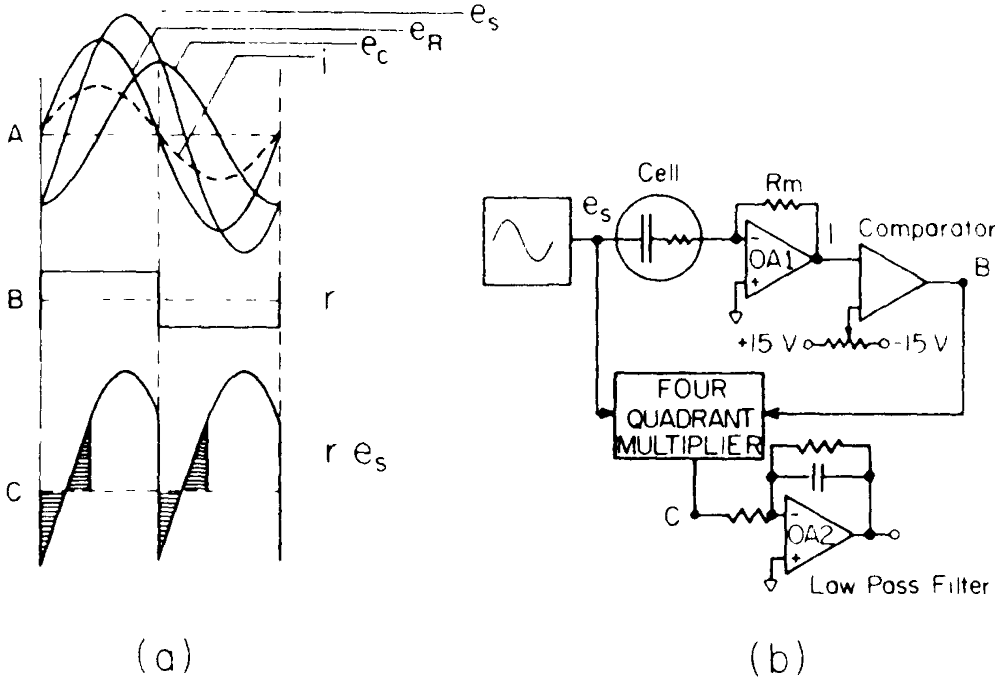

(a) (b)

Figure 8.13 Conductance measurement by phase-selective demodulation: (a) waveforms; (b) circuit schematic.

exercise, the reader may verify that this is true over the second half-cycle and that cross-correlation of e_s with a quadrature square wave results in an integral that is proportional to X_C.

For $r = 1$ over the first half-cycle, the correlation integral is

$$cc = \int_0^\pi (+1)e_s \, dt \tag{8.43}$$

Since e_s may be expressed as the sum of e_R and e_C, we have the following:

$$cc = \int_0^\pi (+1)\left(IR \sin \omega t - \frac{I}{\omega C} \cos \omega t \right) dt \tag{8.44}$$

Separation of the sine and cosine terms gives

$$cc = IR \int_0^\pi \sin \omega t - \frac{1}{\omega C} \int_0^\pi \cos \omega t \tag{8.45}$$

$$= -\left(\frac{IR}{\omega} \cos \omega t \right)_0^\pi - \left(\frac{I}{\omega^2 C} \sin \omega t \right)_0^\pi \tag{8.46}$$

$$= \frac{2I}{\omega} R \tag{8.47}$$

Therefore, the magnitude of the correlation integral is proportional to the resistive component of the cell impedance at constant frequency. This is shown qualitatively in waveforms A to C of Figure 8.13a. Graphical multiplication of waveform B and e_s in A gives the correlation waveform C. The shaded areas represent areas that cancel upon integration and the unshaded area represents $\int re_s \, dt$.

Instrumentally, the cross-correlation and integration may be easily carried out by the circuit shown in Figure 8.13b. The cell is arranged so that it is the input impedance to the familiar current follower. If a sinusoidal voltage e_s is impressed across the cell, the output of operational amplifier OA1 is proportional to and in phase with the current i (see waveform A). Since i is in phase with e_R, we may use the output of OA1 to generate the bipolar square wave of waveform B. This is accomplished by the comparator, which is adjusted so that its output alternates between its positive and negative limits as the current waveform changes sign. The output of the comparator is connected to the four-quadrant multiplier, which carries out the multiplication of the square wave with e_s. The output of the multiplier is then filtered by the active low-pass filter to provide a dc output voltage proportional to R.

Circuitry similar to that presented in Figure 8.13b has been used to analyze cells with impedances ranging from 10^2 to 10^{11} Ω with 1% accuracy and resolution better than 1 part in 10^4 over a frequency range of 0.005 Hz to 10 kHz [14]. The technique has been especially useful for studies of the reaction kinetics of moderately fast chemical reactions. Kadish et al. [15] used phase-selective techniques to make ac impedance measurements to evaluate reference electrodes for use in nonaqueous solvents. Recent decreases in the cost of integrated function modules such as analog multipliers, oscillators, and phase-locked loops make this type of phase-selective instrumentation more accessible than ever.

Traditionally, the instrument of choice for accurate conductance measurements that are relatively free of capacitance effects has been the ac Wheatstone bridge illustrated in Figure 8.14. The details of operation and the derivation of the balance condition of the ac bridge are presented in considerable detail elsewhere [16,17]. The balance condition is exactly analogous to that of the dc bridge except that impedance vectors must be substituted for resistances in the arms of the bridge when reactive circuit elements are present.

At balance, the points at d and b on the ac bridge must be equal in magnitude as well as in phase. The simplest method for determining when this condition exists is to use an oscilloscope connected as shown in the figure as the null detector. If precautions are taken to ensure that the excitation and the null signal are electronically isolated, the balance condition is easily, albeit slowly, obtained [16].

Assuming that the bridge is operated at frequencies for which the parallel capacitance of the cell has negligible conductance, the bridge will balance when $R_s = R_{cell}$ and $C_s = C_{cell}$. Bridges that have been carefully calibrated against known standard resistors may achieve accuracies of 0.01%. With careful prepa-

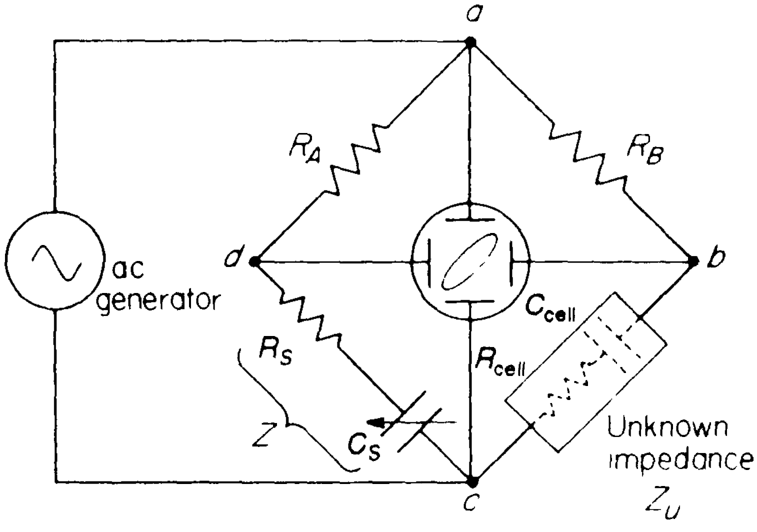

Figure 8.14 Impedance bridge.

ration of solutions and control of experimental conditions, the measurement of conductances by this method ranks among the most accurate and precise of all electrochemical techniques.

C. Bipolar Pulse Measurements

The bipolar pulse technique for measuring solution resistance minimizes the effects of both the series and parallel cell capacitances in a unique way. The instrumentation for this technique is illustrated in Figure 8.15. The technique consists of applying two consecutive voltage pulses of equal magnitude and pulse width but of opposite polarity to a cell and then measuring the cell current precisely at the end of the second pulse [18].

The pulses are provided by a precision bipolar voltage source, which is switched into the input of the pulsing amplifier by the switch at point A in the circuit. A very accurate crystal-controlled timing circuit (not shown) drives the switch to ensure that the pulses are symmetrical. The pulsing amplifier inverts the signal as shown by waveform B and supplies current to the cell. The cell current is amplified by the current follower, the output of which is illustrated by waveform C.

At the beginning of the first pulse, any parallel capacitance in the cell is rapidly charged, producing the small spike in waveform C. As long as $t_1 << R_sC_s$, the potential developed across C_s will be small compared to the excitation potential E_{in}. During t_1, the current will decrease slightly as the poten-

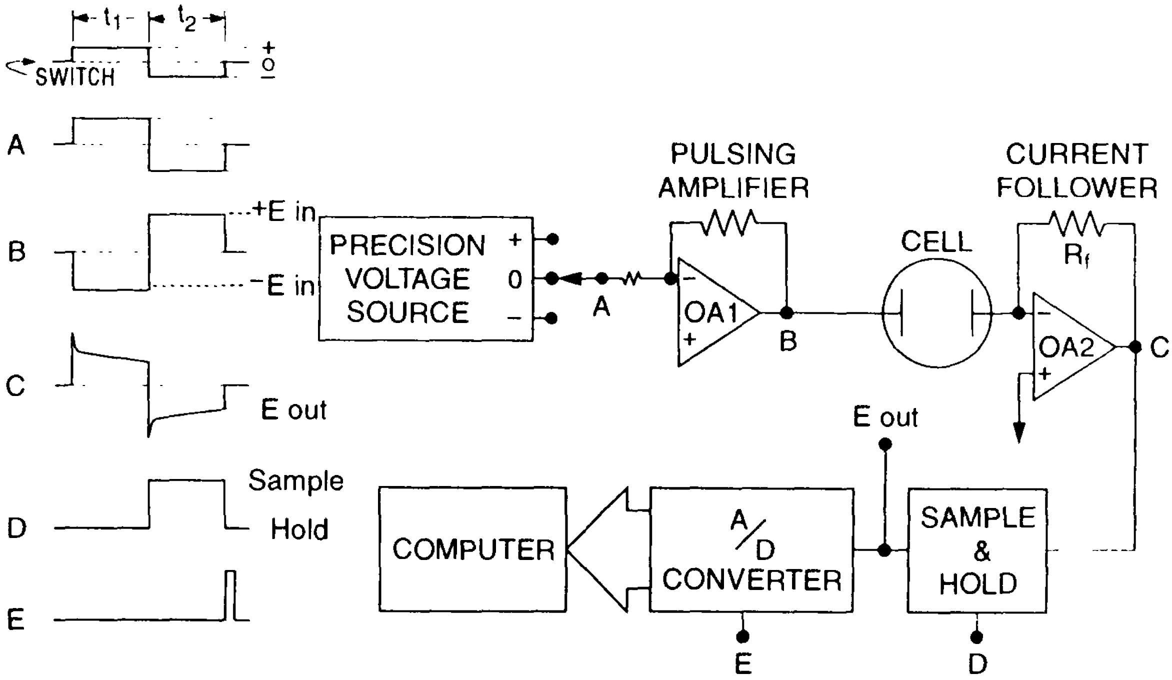

Figure 8.15 Bipolar pulse conductance measurement system.

tial across C_s increases. At the end of the first pulse, the polarity is quickly reversed, again resulting in the small spike due to charging of the parallel capacitance. Assuming that $t_1 = t_2$, the double layer is exactly discharged during the second half of the cycle, and the cell current at the end of t_2 is due to the resistive component of the cell impedance alone.

The sample-and-hold amplifier samples the output of OA2 during t_2 as shown by waveform D and holds the signal E_{out} at the exact end of the second pulse. The falling edge of signal D fires a monostable multivibrator generating a trigger pulse (E) for the analog-to-digital conversion of the sample-and-hold output. Between pulses the cell is held at ground potential in order to eliminate any spurious currents.

The resistance of the cell is calculated from the following expressions. Since, at the end of t_2,

$$i_{cell} = \frac{E_{out}}{R_f} \quad \text{and} \quad R_s = \frac{E_{in}}{i_{cell}} \tag{8.48}$$

we have

$$R_s = \frac{E_{in}}{E_{out}} R_f \tag{8.49}$$

If the pulse widths of the two pulses are equal to within 1% and the double-layer voltage can be kept to less than 1% of the applied voltage by keeping the pulses short (i.e., 10 μs to 10 ms in duration), the conductance may be determined to within 0.01% [18].

The advantages of the bipolar pulse technique include speed (discrete measurements at a rate as high as 30 kHz), accuracy, and signal-to-noise ratio. The system has been employed as a detector in automated conductometric titrations and in stopped-flow mixing systems with excellent results.

In another variation of the bipolar pulse technique, a bipolar current pulse is applied to a conductance cell, and the voltage is sampled at the end of the second pulse [19]. Analogously, the solution resistance is calculated from $R_s = E_{measured}/i_{applied}$. This technique has also been applied with good success to chemical problems similar to those mentioned above.

Applications of the bipolar pulse technique have demonstrated its utility in a variety of experiments, but it is particularly useful in monitoring reaction kinetics [18]. The technique has been shown to be useful on the stopped-flow time scale by the investigation of the dehydration of carbonic acid [20]. The study of this widely used text reaction demonstrates the accuracy and precision of the method. A sample data set from a single experiment is shown in Figure 8.16, and the excellent precision obtainable in such experiments is evident. The

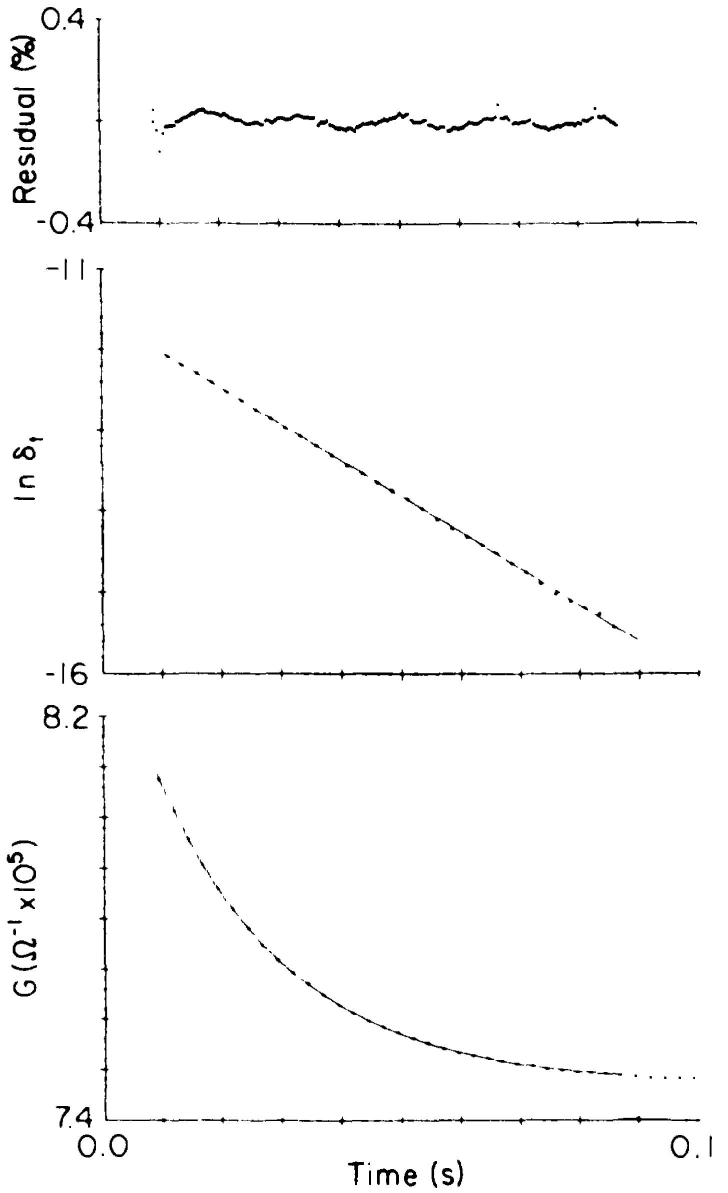

Figure 8.16 Reaction curve for the dehydration of carbonic acid by conductometric detection. Lower: dots, every tenth experimental point; solid line, fitted exponential curve. Middle: dots, logarithmic plot, every tenth point; solid line, least-squares line. Upper: residuals ($G - G_{calcd}$). [From Ref. 20, reprinted with permission. Copyright 1978 American Chemical Society.]

standard error of the estimate of the fitted first-order logarithmic plot (middle curve) amounts to 0.2% of the conductance change or 0.015% of the average conductance during the course of the reaction. Using a computer-controlled instrument with simultaneous measurement of conductance and temperature, it is also possible to correct conductance measurements to constant temperature.

More recently, the kinetics of the urease-catalyzed decomposition of urea were investigated using a wide-range bipolar pulse instrument capable of both current and voltage pulse modes with either integrated or sampled data acquisition [21]. With this instrument, conductance accuracy of 1% was attained over the range of 5×10^{-9} mho to 10 mho. Accuracy of 0.001-0.01% was achieved over the range of 10^{-6} mho to 1 mho while measurements were made in as few as 32 μs.

A novel application of the bipolar pulse technique that introduces a degree of selectivity into conductometric methods is found in the measurement of the conductance of ion-selective electrodes as a means of rapidly measuring ion concentrations [22]. For example, working curves of conductance versus log concentration for Ca^{2+} are linear over at least four decades of concentration with a detection limit of 10^{-6} M. The response time for measuring the conductance of a calcium ion-selective electrode is about 10 ms. Other applications of the bipolar pulse technique, including the measurement of critical micelle concentrations [23] and high-precision conductometric titrations [24], have appeared in the literature, but none is more significant than its use as a detector in ion chromatography [25]. A large fraction of the commercial conductometric detectors for ion chromatography are based on the bipolar pulse method. The advent of the bipolar pulse conductance technique has generated renewed interest in one of our oldest instrumental methods.

REFERENCES

1. J. E. Prue, *Ionic Equilibria*, Topic 15, Vol. 3 of *International Encyclopedia of Physical Chemistry and Chemical Physics*, Pergamon Press, New York, 1966.
2. R. A. Robinson and R. H. Stokes, *Electrolyte Solutions*, 2nd ed., revised, Butterworth, Sevenoaks, Kent, England, 1968.
3. R. M. Fuoss and L. Onsager, *J. Phys. Chem. 66*:1722 (1962); *67*:621 (1963); *68*:1 (1964).
4. H. V. Malmstadt, C. G. Enke, and S. R. Crouch, *Electronics and Instrumentation for Scientists*, Benjamin-Cummings, Menlo Park, CA, 1981, pp. 115-121.
5. H. V. Malmstadt, C. G. Enke, and E. C. Toren, Jr., *Electronics for Scientists*, Benjamin-Cummings, Menlo Park, CA, 1962, pp. 545-581.
6. R. D. Sacks and H. B. Mark, Jr., *Simplified Circuit Analysis*, Marcel Dekker, New York, 1972, Chap. 1.
7. A. G. Diefenderfer, *Principles of Electronic Instrumentation*, 2nd ed., W. B. Saunders, Philadelphia, 1979, Chap. 2.
8. D. F. Evans and M. A. Matesich, in *Techniques of Electrochemistry* (E. Yeager and A. J. Salkind, eds.), Wiley-Interscience, New York, 1973, p. 49.
9. *Ibid.*, p. 30.
10. T. Shedlovsky, in *Techniques of Organic Chemistry*, 2nd ed., Vol. I, Part II (A. Weissberger, ed.), Interscience, New York, 1959.
11. C. N. Reilley, *J. Chem. Educ. 39*:A853 (1962).
12. J. I. Smith, *Modern Operational Circuit Design*, Wiley-Interscience, New York, 1971, Chap. II.
13. Ref. 4, p. 420.

14. A.J. Bentz, J.R. Sandifer, and R.P. Buck, *Anal. Chem. 46*:543 (1974).
15. S. Cai, T. Malinski, X. Lin, J. Ding, and K. M. Kadish, *Anal. Chem. 55*:161 (1983); K. M. Kadish, S. Cai, T. Malinski, J. Ding, and X. Lin, *Anal. Chem. 55*:163 (1983).
16. J. Braunstein and G. D. Robbins, *J. Chem. Educ. 48*:52 (1971).
17. Ref. 1, p. 481.
18. D. E. Johnson and C. G. Enke, *Anal. Chem. 42*:329 (1970).
19. P. H. Daum and D. F. Nelson, *Anal. Chem. 45*:463 (1973).
20. K. J. Caserta, F. J. Holler, S. R. Crouch, and C. G. Enke, *Anal. Chem. 50*:1534 (1978).
21. R. K. Calhoun, F. J. Holler, R. F. Geiger, Jr., T. A. Nieman, and K. J. Caserta, *Anal. Chim. Acta 252*:29 (1991).
22. C. R. Powley and T. A. Nieman, *Sel. Electrode Rev. 10*:185 (1988).
23. J. Baxter-Hammond, C. R. Powley, K. D. Cook, and T. A. Nieman, *J. Colloid Interface Sci. 76*:434 (1980).
24. M. E. Hail and F. J. Holler, *Mikrochim. Acta 111*:295 (1986).
25. J. M. Keller, *Anal. Chem. 53*:344 (1981).